Land-Atmosphere Feedbacks Dampen Surface Evapotranspiration in Wet Regions

Claire M. Zarakas[1*], Abigail L. S. Swann[1,2], and David S. Battisti[1]

[1]Department of Atmospheric Sciences, University of Washington, Seattle, WA 98195
[2]Department of Biology, University of Washington, Seattle, WA 98195

Key Points:

- Land-atmosphere feedbacks dampen ET changes in energy-limited regions and amplify ET changes in some moisture-limited regions.
- Feedbacks between evapotranspiration and vapor pressure deficit drive the robust dampening mechanism in energy-limited regions.
- Offline land models may systematically overestimate water cycle responses, highlighting the need for coupled land model development.

*Now at CarbonPlan and University of California, Irvine

Corresponding author: Claire Zarakas, czarakas@schmditsciencefellows.org

Abstract

Terrestrial processes control land-to-atmosphere fluxes of water, energy, and carbon and are also influenced by climate. Feedbacks in the land-atmosphere coupled system can therefore potentially modulate changes in land surface water fluxes. Prior work has largely focused on one specific aspect of land-atmosphere coupling modulated by soil moisture, while devoting less attention to other ways in which coupling between the land and atmosphere could alter climate. We use a novel experimental design of paired perturbed parameter ensembles in an Earth system model to isolate the extent to which land-atmosphere feedbacks modulate the global water cycle by perturbing land parameters spanning a wide range of terrestrial processes that affect evapotranspiration. We find support for the traditional soil moisture-precipitation coupling in some dry or transitional dry-to-wet regions where evapotranspiration is soil-moisture limited. However, we also find that land-atmosphere feedbacks have a dampening effect on evapotranspiration in wet regions, which is more widespread and robust than the impact in dry regions and is consistent with first principles. By adopting a holistic definition of land-atmosphere coupling, our analysis provides insights into where and how land-atmosphere feedbacks modulate terrestrial processes, posing a challenge to the widespread practice of developing and evaluating land models in an uncoupled configuration and then deploying them to understand and predict terrestrial processes in a coupled context.

Plain Language Summary

The exchange of water, energy, and carbon between the land surface and the atmosphere is driven both by atmospheric conditions and by processes occurring on land. We find that land-to-atmosphere fluxes of water are different when the atmosphere can respond to changes on land, and that the atmosphere acts as an amplifier in some dry places and has a dampening effect in wet places. In dry places this happens because precipitation decreases when soils are dry, while in wet places the atmosphere becomes more moist when it can respond which reduces the evaporative demand of the atmosphere. The dampening effect in wet places is robust and consistent with theory but has been previously underemphasized when interpreting findings from offline experimental designs.

1 Introduction

Terrestrial processes such as photosynthesis and the movement of water through soils influence climate from local to global scales by modifying land-to-atmosphere fluxes of water, energy, and momentum. These processes are also directly influenced by climate due to their dependence on air temperature, relative humidity, net radiation, and soil moisture (SM). The land and atmosphere are therefore a coupled system, in which biogeophysical land-atmosphere feedbacks can modulate changes in land surface water and carbon fluxes. An extensive body of literature has long established mechanisms through which land processes impact the atmosphere (i.e., the land-to-atmosphere branch of this coupled system; Shukla & Mintz 1982, Sellers et al. 1996, Laguë et al. 2019), as well as how the atmosphere impacts land surface fluxes (i.e., the atmosphere-to-land branch; Budyko 1974, Whittaker 1975).

Many prior studies have demonstrated that land-atmosphere feedbacks are important controls on temperature and precipitation (Koster et al. 2004, 2006, Seneviratne et al. 2006, Guo et al. 2006, Seneviratne et al. 2010, Dirmeyer 2011, Dirmeyer et al. 2012, Lorenz et al. 2016). Much of this prior work has focused on SM changes as the underlying driver of land-atmosphere feedbacks, and evaluated the strength of land-atmosphere coupling by analyzing climate modeling experiments that turn on and off SM coupling (i.e., GLACE experiments, Koster et al. 2004, 2006, Guo et al. 2006) or by analyzing the correlation between SM, evapotranspiration (ET), precipitation, and temperature in ob-

servations (Dirmeyer 2011, Wei & Dirmeyer 2012, Tuttle & Salvucci 2016, Abdolghafoorian & Dirmeyer 2021) and models (Dirmeyer et al. 2009, Dirmeyer 2011). This body of work has found that SM-precipitation and SM-temperature feedbacks are strongest in transitional dry-to-wet regions (Koster et al. 2006, Seneviratne et al. 2013), and often identified the North American Great Plains and the Sahel as land-atmosphere coupling hot spots. However, the sign and strength of the SM-precipitation feedback remains an open question. In particular Lee & Hohenegger (2024) found strong positive SM-precipitation coupling in a coarse-resolution model but weaker and largely negative SM-precipitation coupling in a storm-resolving model, highlighting that modeled SM-precipitation feedbacks are likely resolution dependent. Additionally, Guillod et al. (2015) found the sign of SM-precipitation feedbacks can differ when evaluating feedbacks spatially versus temporally. While uncertainties remain, the extensive literature on SM-climate feedbacks has been highly influential in demonstrating that terrestrial processes feed back on the atmosphere and has led to a focus on land-atmosphere feedbacks in transitional dry-to-wet regions.

SM-climate coupling is strongest in transitional regions because two key conditions for SM-climate coupling are met: (1) ET rates (and variation in those rates) are large enough to impact climate, and (2) SM is the primary control on ET (Seneviratne et al. 2010). In this SM-climate coupling framework, land-atmosphere feedbacks are weak in wet regions because ET is energy-limited rather than SM-limited. It is widely recognized within the field that SM is but one aspect of a complex system of interactions between land surface energy and water fluxes, the planetary boundary layer, clouds, and atmospheric circulation (as highlighted in schematics illustrating the complexity of the land atmosphere system, e.g. see Santanello et al. (2018), Ek & Holtslag (2004), van Heerwaarden et al. (2009)). Nonetheless, the SM land-atmosphere feedbacks framework has been so influential that the term "land-atmosphere feedbacks" is often understood to refer only to feedbacks driven by changes in SM, and much of the existing literature has focused on SM's role in land-atmosphere interactions. However, changes in land-to-atmosphere water and energy fluxes also impact the atmosphere in wet regions, and these atmospheric changes have the potential to modulate land ET independent of the SM feedback.

Here, we evaluate additional mechanistic pathways through which terrestrial processes are coupled to the atmosphere. We adopt a broad definition of land-atmosphere feedbacks, in that we consider ET to be the driver of the feedback loop, such that SM is a part of the feedback loop rather than an external driver. A handful of studies have quantified a similar feedback. For example, Laguë et al. (2019) compared coupled and land-only simulations to isolate the impact of land-atmosphere feedbacks on land surface climate, focusing on atmospheric amplification of land-driven temperature changes. However, prior work has focused on idealized changes to land surface properties and specific regional dynamics. We still lack a systematic, quantitative global understanding of how coupled biogeophysical land-atmosphere feedbacks modulate changes in the terrestrial water and carbon cycles.

In this study, we quantify how biogeophysical land-atmosphere feedbacks modulate changes in land water fluxes across both dry and wet regions and on a global scale using a unique paired perturbed parameter ensemble (PPE) experimental design to isolate the atmosphere's role in modulating terrestrial processes. We perturb land parameters spanning a wide range of terrestrial processes in two PPEs: one in which the atmosphere can respond to land surface changes (coupled), and one in which the land is forced with a fixed atmosphere (land-only). By making pairwise comparisons between the coupled and land-only simulations, we are able to directly quantify the impact of land-atmosphere feedbacks. We note that the goal of this study is not to quantify parameter uncertainty, but rather to leverage this PPE dataset to gain mechanistic insights into how land-atmosphere feedbacks modulate changes in terrestrial processes. We ask the following questions: (1) how do land-atmosphere feedbacks modulate land-driven changes

in mean ET, and (2) what mechanisms determine the sign and spatial pattern of these land-atmosphere feedbacks?

By adopting a more holistic perspective on land-atmosphere feedbacks beyond just the SM-climate feedback, we are able to explore land-atmosphere feedbacks' influence on ET in regions that are primarily energy-limited and therefore insensitive to SM changes (e.g. the Amazon and temperate mid-latitudes), allowing us to identify a dampening feedback mechanism which is consistent with theory but has been underemphasized in the traditional land-atmosphere feedback literature.

2 Methods

2.1 Paired perturbed parameter ensembles

We ran paired perturbed parameter ensembles (PPEs) under preindustrial conditions using two configurations of CESM2 (Danabasoglu et al. 2020): a coupled configuration ("coupled") which includes both a land surface and an atmosphere with a slab ocean and an uncoupled, land only configuration ("land-only"), which are described in detail in Zarakas et al. (2024). For both PPEs, we ran one-at-a-time parameter perturbation experiments for 18 land parameters (Table S1), where we perturbed each parameter to a minimum and maximum value (ensemble n = 36) based on plausible parameter ranges determined by the CLM5-PPE project (Kennedy et al. 2025). The parameter selection procedure and model configurations are described in more detail in Zarakas et al. (2024). The 18 parameters we sampled are described in detail in Table S1 and parameterize diverse terrestrial processes, including soil hydrology, photosynthesis, and stomatal conductance. All simulations were run at 1.9° x 2.5° model resolution under preindustrial conditions for 140 years, and the first 40 years were discarded as spin up.

In the coupled PPE, the atmosphere responds to changes in land surface parameters (i.e. land-atmosphere feedbacks are turned on), while in the land-only PPE, the atmospheric state is prescribed at 3-hourly resolution to match the atmosphere simulated in the reference coupled simulation that used default parameters (i.e. land-atmosphere feedbacks are turned off). We can therefore quantify the impact of land-atmosphere feedbacks on terrestrial processes by making pairwise comparisons between each coupled and land-only ensemble member. We exclude all gridcells that contain snow during all months of the average year.

2.2 Disentangling the land-to-atmosphere and atmosphere-to-land branches of land-atmosphere feedbacks

We identify the mechanisms through which land-atmosphere feedbacks modulate changes in land surface processes by decomposing the overall feedback into two branches: the land-to-atmosphere branch and the atmosphere-to-land branch. Land-atmosphere feedbacks can modulate terrestrial processes only when changing land processes impact atmospheric quantities that are inputs to the land model (Table S2). We therefore focus on these quantities, particularly near-surface atmospheric temperature, precipitation, humidity, and surface radiation.

2.2.1 Influence of land-atmosphere feedbacks on ET

We quantify the impact of land-atmosphere coupling on ET by regressing the annual mean ET from the 36 coupled PPE ensemble members against the annual mean ET from the 36 land-only PPE ensemble members at each model land grid box. Results are shown in Figure 1. When displaying results in climate space, results are binned by annual mean temperature and precipitation and only climate bins that contain greater than 10 gridcells are shown. When displaying results in Budyko space, ET, R_{net}, and P (as

in Figure 1c) are from the coupled reference case. We adopt the null hypothesis that land-atmosphere feedbacks do not modulate changes in land surface fluxes (i.e., in each grid cell that $\Delta ET_{coupled} = \Delta ET_{land-only}$, or in the context of the linear regression, that the slope equals 1). We apply ordinary least squares regression across ensemble members, such that each data point represents the multi-year mean response of a single perturbed-parameter simulation. We perform this analysis at each land grid cell and report changes as being statistically significant after controlling for a false discovery rate of 0.05 (Wilks 2016).

2.2.2 Isolating how land surface fluxes impact the atmosphere

We use ordinary least squares regression to quantify the sensitivity of atmospheric state variables to changes in ET. First, we calculate the gridded changes in annual mean ET from the reference case for each ensemble member. We then regress coupled changes in atmospheric state variables on the ET changes from the paired land-only model experiments in order to isolate the land-to-atmosphere branch of the land-atmosphere feedback. In the coupled PPE, changes in ET are due to both land parameter changes and atmospheric changes (e.g., ET changes driven by changes in precipitation, temperature, etc.), but in the land-only PPE, ET changes are only due to land surface parameter perturbations. We define the sensitivity of atmospheric state variables to changes in ET as the slope of the regression. For example, we calculate the precipitation sensitivity to ET ($\frac{\partial P_{coupled}}{\partial ET_{land-only}}$) by regressing coupled changes in precipitation against land-only changes in ET for each grid cell across the 36 PPE ensemble members. We note that in the coupled context, both local and remote land surface changes can impact the atmosphere in a given grid cell, and we discuss remote effects in Supplemental Text 1. We calculate potential evapotranspiration as in Supplemental Text 2.

2.2.3 Isolating how atmospheric changes impact land surface fluxes

We identify how changes in atmospheric quantities influence land surface fluxes by running additional idealized land-only simulations. We ran idealized land-only simulations where we modified the atmospheric quantities that impact the land (Table S3). This method allows us to quantify the terrestrial response to mean state climate changes, but does not illuminate the terrestrial response to shorter timescale atmospheric variability, which land parameter perturbations can also impact. From these simulations, we calculate the land sensitivity to each meteorological driver (e.g. the sensitivity of ET to precipitation change is $\frac{\partial ET}{\partial P}$).

2.2.4 Decomposing the influence of land-atmosphere feedbacks upon ET

We then quantify the extent to which different atmospheric quantities X contribute to the overall fractional change in ET due to land-atmosphere feedbacks ($\Delta ET_{feedback}$) using Equation 1:

$$\Delta ET_{feedback} = \sum_{X} \left(\frac{\partial X_{coupled}}{\partial ET_{land-only}} \frac{\partial ET}{\partial X} \right), \tag{1}$$

where $\frac{\partial X_{coupled}}{\partial ET_{land-only}}$ is the sensitivity of atmospheric quantity X to changes in ET (as diagnosed through regression, section 2.2.2), and $\frac{\partial ET}{\partial X}$ is the sensitivity of ET to changes in atmospheric quantity X (as diagnosed through idealized meteorology simulations using the land-only model configuration, section 2.2.3). This decomposition assumes linear independence between changes in the atmospheric forcing variables, which is true for $\frac{\partial ET}{\partial X}$ but an imperfect assumption for $\frac{\partial X_{coupled}}{\partial ET_{land-only}}$ (e.g., increasing precipitation may be correlated with increasing near-surface specific humidity). We sum over the equilibrium annual averages of the major atmospheric inputs X to the land model: temperature at the lowest atmospheric level, total precipitation, specific humidity at the lowest atmospheric level, incident solar radiation, and incident longwave radiation. We perform this

analysis using annual mean quantities, rather than seasonally resolved ones, in order to ease comparison across latitudes with varying degrees of seasonality. We note that land–atmosphere interactions vary seasonally, and we expect feedbacks to be strongest during the growing season.

3 Results and Discussion

3.1 Land-atmosphere feedbacks modulate ET

We quantify the net land-atmosphere feedback by regressing mean ET in the 36 member coupled PPE against the mean ET in the 36 paired simulations in the land-only PPE. We find that land-atmosphere feedbacks substantially modulate ET changes, and that the sign of the impact of land-atmosphere feedbacks varies spatially (Figure 1a) depending on the climatological moisture regime. Consistent with prior coarse resolution climate modeling studies, we find that in climatologically dry and transitional dry-to-wet regions land-atmosphere feedbacks either amplify ET changes or are not statistically significant (Figure 1a-b). We also find that in climatologically wet regions land-atmosphere dampen land-driven changes in ET (Figure 1a-b). In the Budyko framework (Budyko 1974), this corresponds to dampening land-atmosphere feedbacks in energy-limited locations where there is more annual precipitation than energy available to evaporate it and amplifying feedbacks or no feedbacks in moisture-limited locations where ET is instead controlled by water availability (Figure 1c). The magnitude of this atmospheric modulation is significant, particularly in the energy-limited regime, where land-atmosphere feedbacks can dampen ET changes by 20 to 60%.

ET differs between the land-only and coupled PPEs because land-atmosphere feedbacks modulate land responses to global-scale land parameter perturbations. Our goal in this study is to quantify the impact of global-scale land-atmosphere feedbacks on land surface fluxes, and to identify where, and through what mechanisms, land-atmosphere feedbacks lead ET to respond differently in a coupled context than in a land-only context. We use the fraction of variance explained by local regression with land-only ET changes as a proxy for the extent to which local to regional ET changes are responsible for the observed land-atmosphere feedbacks (see Supplemental Text 1 for discussion of remote impacts). In many tropical and temperate humid to semi-arid regions, local regression explains a large fraction of variance across the coupled PPE, suggesting a dominant role of local to regional land surface changes (Figure S1e).

In the global average, land-atmosphere feedbacks slightly dampen global mean changes in ET (by 14% on average, Figure S2a) because most of the Earth's ET occurs in wet regions, so the wet regime land-atmosphere feedbacks dominate the global signal. This dampening effect in the global mean highlights a discrepancy between prior work on land-atmosphere feedbacks which has largely focused only on amplifying regions which are climatologically dry, despite the widespread role of land-atmosphere feedbacks in climatologically wet regions.

3.2 Mechanisms controlling land-atmosphere feedbacks

The impact of land-atmosphere feedbacks on ET varies depending on the climatological water regime because changing land ET impacts multiple atmospheric quantities simultaneously, and the climatological water regime determines which atmospheric changes exert the strongest control on ET at that location (Figure 1d). We can see this climatological dependence clearly in idealized simulations where we modify temperature and precipitation independently (Figure 2). Increasing precipitation increases ET, with the largest ET increases occurring in moisture-limited locations (Figure 2a,c). Increasing temperature also increases ET, and conversely decreasing temperature decreases ET, but changes in temperature have the largest impact in energy-limited locations (Figure

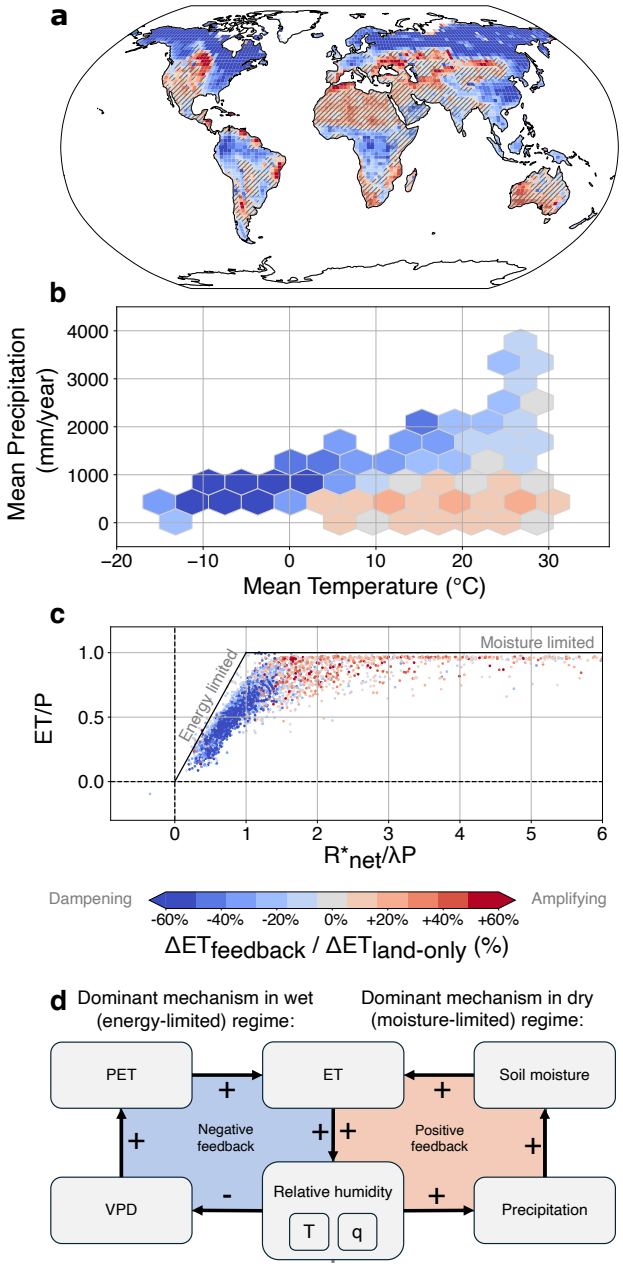

Figure 1. Influence of land-atmosphere feedbacks on land ET. Influence of land-atmosphere feedbacks on ET, as calculated by the regression between coupled and land-only changes in ET (a) spatially, (b) averaged in each mean climate space (T, P), and (c) in the Budyko energy- and moisture-limited framework $R^*_{net}/\lambda P$ vs. ET/P (Budyko 1974). Reds indicate regions where land-atmosphere feedbacks amplify changes in ET, and blues indicate regions where land-atmosphere feedbacks dampen changes in ET. Stippling in (a) indicates regions where the slope is not statistically significantly different from 1. In (c), the grid cell values shown in (a) are plotted in relation to the Budyko framework, where black lines indicate theoretical energy limits ($\lambda ET = R^*_{net}$) and moisture limits ($ET = P$) on ET, where P is the precipitation rate, λ is the latent heat of evaporation, and R^*_{net} is net radiation minus ground heat flux. The dampening category extends beyond 1.0 because we plot grid cells using the original Budyko (1974) definition of the aridity index based on R^*_{net} instead of potential evapotranspiration, and in reality land's ability to evaporate water also depends on additional factors such as vapor pressure deficit and evaporative resistance. Schematic of dominant land-atmosphere feedbacks on an initial ET perturbation by climatological moisture regime (d). The sign of the feedback on the initial ET perturbation is found by multiplying the signs in the feedback loop.

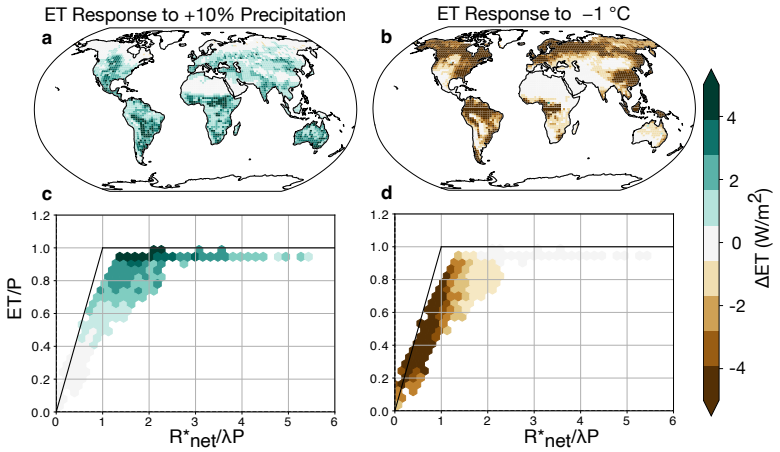

Figure 2. How atmospheric changes impact ET. ET response to idealized meteorological treatments of (a) increasing precipitation and (b) decreasing temperature. The idealized meteorological treatments are described in section 2.2.3. The bottom row bins the ET responses to increasing precipitation (c) and decreasing temperature (d) in the Budyko framework. ET, P, and R^*_{net} which define the Budyko space in panels (c) and (d) are from the reference simulation. The coupled and land-only reference simulations are identical because the land-only PPE is forced with the meteorology from the coupled reference case. ET is normalized by the magnitude of precipitation change in Figure S3.

2b,d) because increasing temperature while maintaining constant specific humidity increases the atmospheric demand for moisture due to the Clausius-Clapeyron relationship.

As has been previously established in the literature, atmospheric responses amplify ET changes in some dry regions where (1) increasing ET increases precipitation, and (2) ET is moisture-limited and therefore more sensitive to precipitation changes (Figure 1d). Increasing ET increases modeled precipitation in some regions (Figure 3a), likely due to a combination of local land-atmosphere coupling (e.g. as is typical in the Great Plains) and larger scale circulation responses (e.g. asymmetric precipitation responses to ET reductions as in Kooperman et al. (2018), shifts in the inter-tropical convergence zone as in Laguë, Swann, & Boos (2021), or impacts on planetary waves as in Koster et al. (2016)). Precipitation increases can increase SM, thereby amplifying the initial ET increase. However, land-atmosphere feedbacks do not amplify ET changes in all dry or transitional locations because increasing ET does not increase precipitation in all of these regions. There are also some regions (e.g., the Amazon) where increasing ET increases precipitation, but does not lead to an amplifying feedback because ET is relatively insensitive to precipitation changes in wet regions.

We find that a different mechanistic pathway dominates in energy-limited regions. Land-atmosphere feedbacks dampen ET changes in energy-limited regions because (1) increasing ET decreases the atmospheric demand for moisture and (2) ET in these regions is limited by the atmospheric demand for water and energy available to evaporate water (i.e., the potential ET, PET), rather than by water availability (Figure 1d). An initial increase in ET decreases PET (Figure 3b) primarily by decreasing the vapor pressure deficit (Figure 3c), which is the atmospheric demand for moisture. This VPD decrease is largely driven by the fact that increasing ET cools the near-surface air (Figure 3c). This leads to global increases in near-surface relative humidity and decreases the vapor pressure deficit (Figure S4g-h). This decrease in the atmospheric demand for

moisture dampens the initial ET change in regions where ET rates are primarily controlled by atmospheric demand. Our results suggest that the negative ET-VPD feedback is primarily due to a decrease in the surface-to-atmosphere moisture gradient that dampens ET changes. However, we note that the ET response could also be modulated by changes in surface conductance. For example, decreased VPD could enhance plant growth (leading to increased leaf area) or increase stomatal conductance, both of which would lead to greater surface conductance. These biotic responses are also captured in our estimate of how atmospheric changes impact ET (Figure S4). However, our results suggest that these plant processes are of second-order importance, since they would lead to a positive ET-VPD feedback (i.e., increasing ET leads to lower VPD, which in turn increases ET), while we observe a negative ET-VPD feedback. VPD (and consequently, PET) also decreases in water-limited regions, but in those locations this change in atmospheric demand influences ET less because ET is controlled primarily by water availability (precipitation) rather than by atmospheric demand for water. We assume that the boundary between energy-limited and water-limited regimes remains constant across our PPE because simulations were all run under constant preindustrial conditions, but we note that the boundary between regimes can also shift under changing climates (Hsu & Dirmeyer 2023).

Increasing ET also drives radiative changes (Figure S5) due to changes in surface temperature, near-surface air temperature, and cloud cover (consistent with Teuling et al. 2017, Zarakas et al. 2020, J. E. Kim et al. 2020). When ET increases, outgoing longwave radiation (Figure S5b) decreases with decreasing surface temperature through the Planck feedback. This decrease in outgoing longwave radiation is partially offset by decreases in downwelling longwave radiation (Figure S5a), due to cooling of the boundary layer driven by both decreased sensible heating and by decreased longwave radiation associated with surface cooling (Vargas Zeppetello et al. 2019). The downwelling longwave response suggests that increasing ET does not necessarily increase water vapor in the full atmospheric column, because the water vapor feedback is initiated by ET-driven surface cooling (Laguë et al. 2023). These longwave changes result in an overall increase in net longwave radiation at the land surface, meaning that the surface is losing less heat (Figure S5c). Increasing ET also decreases downwelling shortwave radiation due to increases in cloud cover (Figure S5d). Reflected downwelling shortwave radiation changes (Figure S5e) are small and vary regionally, due to a combination of downwelling shortwave changes and minor LAI and soil-related albedo changes. On balance, downwelling shortwave changes are larger than reflected shortwave changes, leading to a net decrease in absorbed downwelling shortwave (Figure S5f). When combining both longwave and shortwave radiative changes, individual components partially cancel each other out, leading to a relatively small change in net absorbed radiation (R^*_{net}, Figure S5g) and therefore only minor net radiation-driven changes in PET (Figures 3c, S4d), despite larger changes in individual radiative fluxes.

We can attribute the overall land-atmosphere feedback on ET to the contributions of individual atmospheric variables by multiplying estimates of land-to-atmosphere (Methods, 2.2.2) and atmosphere-to-land (Methods, 2.2.3) branches of the coupled land-atmosphere system. For example, the contribution due to the change in precipitation is found by combining the maps in Figures 3a and 2a (Methods, B.5). We find that the linear combination of the contributions of just temperature and precipitation (Figures 4b and 4c) captures the actual atmospheric modulation reasonably well (compare Figure 4a and Figure 1a), including the emergent dependence on the climatological moisture regime. In particular, we note that precipitation is the dominant driver in moisture-limited regions which show amplifying land-atmosphere feedbacks, while temperature (and therefore PET) is the dominant driver in energy-limited regions which show atmospheric dampening. This supports our mechanistic explanation for the processes controlling land atmosphere feedbacks (Figure 1d) and further highlights the spatially dominant role of land-atmosphere feedbacks in dampening ET responses in wet regions.

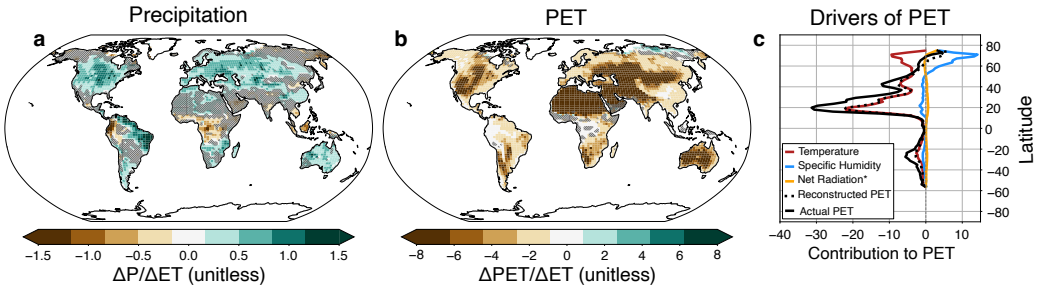

Figure 3. How ET influences the atmosphere. Sensitivity of (a) precipitation and (b) PET to an initial ET perturbation in the coupled model, quantified by linear regression (section 2.2.2). Positive values indicate that increasing ET increases the atmospheric variable. Stippling indicates regions where the slope is not statistically significantly different from 0. (c) quantifies how much the global land mean PET response to an ET perturbation is driven by changes in air temperature, specific humidity, and net radiation. Maps of the sensitivity of temperature, specific humidty, relative humidity, and vapor pressure deficit to changes in ET are in Figure S4.

3.3 A broader definition of land-atmosphere feedbacks

The amplifying land-atmosphere feedback mechanism we identified in moisture-limited regions is consistent with the SM feedbacks literature, though SM forcing studies quantify land-atmosphere feedbacks in an alternative framework. The canonical land-atmosphere feedback literature adopts a framework where SM is the driver, and the metric of interest is the strength of coupling between SM and precipitation (i.e., $SM_{coupling} = \frac{\partial P}{\partial SM}$) or temperature. This coupling strength can be decomposed into the terrestrial contribution ($\frac{\partial ET}{\partial SM}$) and the atmospheric contribution ($\frac{\partial P}{\partial ET}$), such that $SM_{coupling} = \frac{\partial P}{\partial SM} = \frac{\partial ET}{\partial SM}\frac{\partial P}{\partial ET}$. Analysis of GLACE experiments and observations identify transitional dry-to-wet SM regions to be regions of strong SM-precipitation coupling (Koster et al. 2006, Seneviratne et al. 2013), which align with the regions we identified in this study where coupling with the atmosphere enhances perturbations in ET compared to land-only perturbations (Figure 1).

Here we are quantifying a different kind of land-atmosphere feedback, defined as the modulation of ET by all atmospheric responses to an initial ET change. In this definition, we consider ET to be the driver of the feedback loop, such that SM is a part of the feedback loop rather than an external driver. For example, consider a water-limited location that is unaffected by changes in VPD or net radiation. We quantify the atmospheric modulation of long-term ET changes as $\frac{\partial P_{coupled}}{\partial ET_{land-only}}\frac{\partial ET}{\partial P}$, which can be further decomposed into $\frac{\partial P_{coupled}}{\partial ET_{land-only}}\frac{\partial SM}{\partial P}\frac{\partial ET}{\partial SM}$. Our atmospheric modulation metric therefore has the SM coupling strength embedded in it, but is quantifying a different feedback. Our analysis also differs from the traditional land-atmosphere feedback literature in that many (though not all) land-atmosphere feedback papers focus on daily to interannual variability in SM, ET, and precipitation, while we are focusing on atmospheric modulation of long-term (climatological) changes in land water fluxes.

The negative feedback we identify in wet regions builds on a body of prior work that has extended beyond SM as the main driver of land–atmosphere interactions. For example, van Heerwaarden et al. (2009) develop a mathematical framework for land-atmosphere interactions that includes the negative moistening feedback, wherein ET increases atmospheric specific humidity, which in turn reduces ET. Laguë et al. (2019) discuss the impact of atmospheric feedbacks on ET in a global mean sense, and note that increasing evaporative resistance drives larger changes in ET in land-only simulations than in

coupled simulations. They hypothesize that this is because reductions in ET increase the atmospheric demand for water in coupled simulations, which is consistent with the mechanism that we demonstrate here for energy-limited regions.

Zhou & Yu (2025) and D. Kim & Choi (2026) similarly demonstrate that warming-driven ET changes are overestimated in land-only hydrological models compared to coupled simulations because land-only hydrological models neglect ET's influence on evaporative demand. This ET-VPD feedback mechanism also relates to Decker et al. (2017)'s study on how land-atmosphere feedbacks impact irrigation demand, which found that land-atmosphere feedbacks dampen irrigation demand because irrigation increases ET, which moistens the boundary layer and thereby reduces the atmospheric demand for moisture. Our findings are consistent with this prior work, and extend it by using a novel method to explicitly quantify the full feedback through which atmospheric responses modulate changes in land ET including both wet and dry regions.

Our finding that the sign of overall ET-atmosphere feedbacks depends on the climatological moisture regime also echoes prior studies documenting where specific land-atmosphere feedback mechanisms are positive or negative. For example, feedbacks between SM and triggering of convection are strongly positive in wet regions, and can be negative in dry regions (Findell & Eltahir 2003a,b, Findell et al. 2011, Zhang et al. 2023).

Additionally, the land-to-atmosphere and atmosphere-to-land branches of our identified feedback mechanism are both supported by first principles. The fact that precipitation would have a bigger impact on ET in moisture-limited regions and that VPD would have a bigger impact on ET in energy-limited regions follows from the long-established Budyko framework. More recently, studies emphasizing VPD control on ET (Massmann et al. 2019) have further underscored that atmospheric demand is an important component of land–atmosphere coupling. Similarly, on local scales the surface energy budget requires that increasing ET decreases land surface temperatures, which is the dominant driver of VPD declines in our simulations. Multiple studies have demonstrated that this relationship between ET and temperature holds true in a coupled context on regional to global scales (Shukla & Mintz 1982, Laguë et al. 2019, Kong et al. 2023) and that decreasing ET increases near-surface VPD (Lemordant et al. 2018) under modern continental configurations (though see Laguë, Pietschnig, et al. 2021). The imprint of ET on near-surface temperature and humidity is in fact what enables ET estimation from weather station data (McColl & Rigden 2020, Gentine et al. 2016, Rigden & Salvucci 2015, McColl et al. 2019, Salvucci & Gentine 2013). In the results presented here, we show ET's influence on the atmospheric state directly and explicitly, and extend this concept one step further by quantifying the extent to which that atmospheric response feeds back on ET itself.

Our definition of land-atmosphere feedbacks can also be used to quantify atmospheric modulation of any terrestrial process. In particular, ET and gross primary production (GPP) are tightly coupled, so one might expect that because land-atmosphere feedbacks modulate ET they would also modulate GPP. However, we find that atmospheric modulation of photosynthesis differs from atmospheric modulation of ET in several key ways. Unlike for water fluxes, land-atmosphere feedbacks do not consistently amplify or dampen photosynthesis changes, but they remain important in regional hotspots in the Amazon and the North American Great Plains (discussed in more detail in Supplemental Text 3). This analysis does not assume that land models accurately represent photosynthetic responses to global change, as this remains uncertain. Rather, it sheds light on how land–atmosphere feedbacks alter modeled photosynthesis relative to land-only simulations, which has implications for how results from offline land model studies should be interpreted.

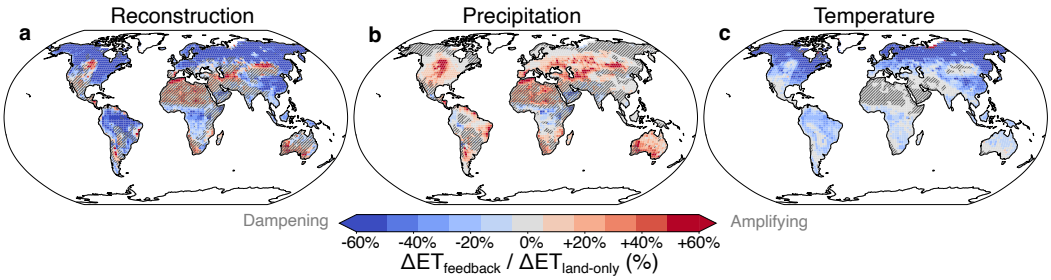

Figure 4. Linear decomposition of the atmospheric modulation of ET changes. (a) Spatial pattern of the atmospheric modulation of ET estimated by summing the contributions due to (b) precipitation, (c) temperature, and other atmospheric quantities shown in Figure S6 (see methods 2.2.4). The total land-atmosphere feedback is directly comparable to the net feedback shown in Figure 1a. Changes are percent changes relative to the change in ET seen in the ensemble of PPE experiments using the land-only model; positive values indicate a positive (amplifying) land-atmosphere feedback. Other atmospheric quantities (specific humidity, downwelling shortwave, and downwelling longwave) have a smaller impact on land-atmosphere feedbacks and are shown in Figure S6.

4 Conclusions and Implications

We leveraged a paired Earth system model PPE to quantify how land-atmosphere feedbacks modulate changes in water and carbon fluxes. Consistent with prior work, we find that land-atmosphere feedbacks can amplify ET through SM-precipitation coupling in some moisture-limited regions. We also found evidence for a widespread and robust land-atmosphere feedback in energy-limited regions, where land-atmosphere feedbacks substantially dampen ET changes.

By adopting a more holistic perspective on land-atmosphere feedbacks beyond just the SM-ET-precipitation feedback, we are able to explore land-atmosphere feedbacks' influence on ET in regions that are primarily energy limited and therefore insensitive to SM changes, allowing us to clearly demonstrate the dampening feedback mechanism. The mechanism which we have explicitly demonstrated is supported by longstanding theory but remains underemphasized in some traditional land-atmosphere feedback literature. Because we used a coarse resolution climate model to run our simulations, the spatial pattern and magnitude of the moisture-limited land-atmosphere feedback is likely model dependent and may suffer from inaccurate SM influences on precipitation in coarse resolution climate models (e.g., Lee & Hohenegger 2024). The SM-precipitation feedback identified in our simulations should therefore be considered a model diagnosis rather than necessarily reflective of SM-precipitation feedbacks in the real world. However, we hypothesize that the energy-limited feedback we identify here is robust across model resolutions because it does not depend on precipitation, a parameterized and non-linear process that is highly resolution dependent.

Furthermore, our paired PPE approach can be applied across models to systematically diagnose land–atmosphere interactions and feedback pathways in a way that is not possible from observations or single-simulation experiments alone. Because the real Earth system does not provide counterfactual realizations in which land–atmosphere feedbacks are turned off, observational studies can disentangle components of land-atmosphere feedbacks, but cannot directly isolate the full atmospheric modulation of land surface processes.

Our finding that land-atmosphere feedbacks modulate ET changes poses a challenge to the widespread practice of developing and evaluating land models in a land only configuration and then deploying them to understand and predict terrestrial processes in a coupled context. Our results indicate that assessing parameters' impact on the water cycle in a land only framework will yield the wrong answer – overestimating parameters' impact on ET by up to 60% in wet regions and underestimating parameters impact in some dry regions. This finding highlights the need to develop global climate models in a coupled context, an approach which other studies have also called for (Dirmeyer et al. 2018, Findell et al. 2024) but which remains uncommon in practice.

Our study specifically quantifies how land-atmosphere feedbacks modulate the impact of land parameter uncertainty, and we use this to generate more general insights into how land-atmosphere feedbacks modulate any land surface perturbation which alters ET (e.g. due to land cover change or changes in plant functioning). For example, our study suggests that land-only experiments will overestimate the impact of CO_2-driven stomatal closure on ET in wet regions, but underestimate it in dry regions. This work also has implications for the assessment of climate change impacts on water resources and terrestrial ecosystems, as independently highlighted by recent studies focusing on PET (Zhou & Yu 2025, D. Kim & Choi 2026). Climate change impacts are often evaluated by running land models in an offline 'land-only' framework that does not account for land-atmosphere feedbacks, but our results show that land-atmosphere feedbacks are strong enough that they can meaningfully change the answer. This expands our fundamental understanding of land-atmosphere feedbacks, and highlights the role of the land surface as an integral part of the coupled Earth system.

Open Research Section

The data and code used in this article are available through the Dryad Digital Repository. Zarakas & Swann (2026a) contains model output and code for the coupled PPE, Zarakas & Swann (2026b) contains model output and code for the land-only PPE, and Zarakas & Swann (2025) contains model output and code for the synthetic meteorology simulations.

Author Contributions

CMZ and ALSS conceptualized the research project, developed the methodology, and administered the project. CMZ ran model experiments, developed code used in this research, performed analysis, prepared visualizations, and wrote the original draft. ALSS and DSB reviewed and edited writing. ALSS supervised the project and provided computing resources.

Acknowledgments

CMZ was supported by the U.S. Department of Energy (DOE) Computational Science Graduate Fellowship (DE-SC0020347). ALSS and CMZ were also supported by the DOE Office of Biological and Environmental Research Regional and Global Model Analysis Program (DE-SC0021209) and the National Science Foundation AGS-1553715 to the University of Washington. The Computational and Information Systems Laboratory at NCAR provided computing and data storage resources, including the Cheyenne supercomputer (`https://doi.org/10.5065/D6RX99HX`). We thank all scientists, software engineers, and administrators who contributed to CESM2's development.

References

Abdolghafoorian, A., & Dirmeyer, P. A. (2021). Validating the land–atmosphere

coupling behavior in weather and climate models using observationally based global products. *Journal of Hydrometeorology*, *22*(6), 1507–1523. doi: 10.1175/JHM-D-20-0183.1

Budyko, M. I. (1974). *Climate and Life* (Tech. Rep.). New York: Academic Press.

Danabasoglu, G., Lamarque, J.-F., Bacmeister, J., Bailey, D. A., DuVivier, A. K., Edwards, J., ... Strand, W. G. (2020). The Community Earth System Model version 2 (CESM2). *Journal of Advances in Modeling Earth Systems*, *n/a*(n/a). doi: 10.1029/2019MS001916

Decker, M., Ma, S., & Pitman, A. (2017). Local land–atmosphere feedbacks limit irrigation demand. *Environmental Research Letters*, *12*(5), 054003. doi: 10.1088/1748-9326/aa65a6

Dirmeyer, P. A. (2011). The terrestrial segment of soil moisture–climate coupling. *Geophysical Research Letters*, *38*(16). doi: 10.1029/2011GL048268

Dirmeyer, P. A., Cash, B. A., Kinter, J. L., Stan, C., Jung, T., Marx, L., ... Manganello, J. (2012). Evidence for Enhanced Land–Atmosphere Feedback in a Warming Climate. doi: 10.1175/JHM-D-11-0104.1

Dirmeyer, P. A., Gentine, P., Ek, M. B., & Balsamo, G. (2018). Land Surface Processes Relevant to S2S Prediction. In *Sub-Seasonal to Seasonal Prediction: The Gap Between Weather and Climate Forecasting*.

Dirmeyer, P. A., Schlosser, C. A., & Brubaker, K. L. (2009). Precipitation, Recycling, and Land Memory: An Integrated Analysis. doi: 10.1175/2008JHM1016.1

Ek, M. B., & Holtslag, A. a. M. (2004). Influence of Soil Moisture on Boundary Layer Cloud Development.

Findell, K. L., & Eltahir, E. A. B. (2003a). Atmospheric Controls on Soil Moisture–Boundary Layer Interactions. Part I: Framework Development. *Journal of Hydrometeorology*, *4*(3), 552–569. doi: 10.1175/1525-7541(2003)004⟨0552:ACOSML⟩2.0.CO;2

Findell, K. L., & Eltahir, E. A. B. (2003b). Atmospheric Controls on Soil Moisture–Boundary Layer Interactions. Part II: Feedbacks within the Continental United States. *Journal of Hydrometeorology*, *4*(3), 570–583. doi: 10.1175/1525-7541(2003)004⟨0570:ACOSML⟩2.0.CO;2

Findell, K. L., Gentine, P., Lintner, B. R., & Kerr, C. (2011). Probability of afternoon precipitation in eastern United States and Mexico enhanced by high evaporation. *Nature Geoscience*, *4*(7), 434–439. doi: 10.1038/ngeo1174

Findell, K. L., Yin, Z., Seo, E., Dirmeyer, P. A., Arnold, N. P., Chaney, N., ... Santanello Jr., J. A. (2024). Accurate assessment of land–atmosphere coupling in climate models requires high-frequency data output. *Geoscientific Model Development*, *17*(4), 1869–1883. doi: 10.5194/gmd-17-1869-2024

Gentine, P., Chhang, A., Rigden, A., & Salvucci, G. (2016). Evaporation estimates using weather station data and boundary layer theory. *Geophysical Research Letters*, *43*(22), 11,661–11,670. doi: 10.1002/2016GL070819

Guillod, B. P., Orlowsky, B., Miralles, D. G., Teuling, A. J., & Seneviratne, S. I. (2015). Reconciling spatial and temporal soil moisture effects on afternoon rainfall. *Nature Communications*, *6*(1), 6443. doi: 10.1038/ncomms7443

Guo, Z., Dirmeyer, P. A., Koster, R. D., Sud, Y. C., Bonan, G., Oleson, K. W., ... Xue, Y. (2006). GLACE: The Global Land–Atmosphere Coupling Experiment. Part II: Analysis. *Journal of Hydrometeorology*, *7*(4), 611–625. doi: 10.1175/JHM511.1

Hsu, H., & Dirmeyer, P. A. (2023). Uncertainty in Projected Critical Soil Moisture Values in CMIP6 Affects the Interpretation of a More Moisture-Limited World. *Earth's Future*, *11*(6), e2023EF003511. doi: 10.1029/2023EF003511

Kennedy, D., Dagon, K., Lawrence, D. M., Fisher, R. A., Sanderson, B. M., Collier, N., ... Wood, A. W. (2025). One-at-a-Time Parameter Perturbation Ensemble of the Community Land Model, Version 5.1. *Journal of Advances in Modeling Earth Systems*, *17*(8), e2024MS004715. doi: 10.1029/2024MS004715

Kim, D., & Choi, M. (2026). A structural correction to atmospheric evaporative demand narrows the gap between offline aridity diagnostics and Earth system model projections. *npj Climate and Atmospheric Science*, *9*(1), 34. doi: 10.1038/s41612-025-01306-3

Kim, J. E., Laguë, M. M., Pennypacker, S., Dawson, E., & Swann, A. L. S. (2020). Evaporative resistance is of equal importance as surface albedo in high-latitude surface temperatures due to cloud feedbacks. *Geophysical Research Letters*, *47*(4), e2019GL085663. doi: 10.1029/2019GL085663

Kong, W., McKinnon, K. A., Simpson, I. R., & Laguë, M. M. (2023). Understanding responses of summer continental daily temperature variance to perturbations in the land surface evaporative resistance. *Journal of Climate*, *36*(6), 1653–1678. doi: 10.1175/JCLI-D-21-1011.1

Kooperman, G. J., Chen, Y., Hoffman, F. M., Koven, C. D., Lindsay, K., Pritchard, M. S., ... Randerson, J. T. (2018). Forest response to rising CO2 drives zonally asymmetric rainfall change over tropical land. *Nature Climate Change*, *8*(5), 434–440. doi: 10.1038/s41558-018-0144-7

Koster, R. D., Chang, Y., Wang, H., & Schubert, S. D. (2016). Impacts of Local Soil Moisture Anomalies on the Atmospheric Circulation and on Remote Surface Meteorological Fields during Boreal Summer: A Comprehensive Analysis over North America.
doi: 10.1175/JCLI-D-16-0192.1

Koster, R. D., Dirmeyer, P. A., Guo, Z., Bonan, G., Chan, E., Cox, P., ... Yamada, T. (2004). Regions of Strong Coupling Between Soil Moisture and Precipitation. *Science*, *305*(5687), 1138–1140. doi: 10.1126/science.1100217

Koster, R. D., Sud, Y. C., Guo, Z., Dirmeyer, P. A., Bonan, G., Oleson, K. W., ... Xue, Y. (2006). GLACE: The Global Land–Atmosphere Coupling Experiment. Part I: Overview. *Journal of Hydrometeorology*, *7*(4), 590–610. doi: 10.1175/JHM510.1

Laguë, M. M., Bonan, G. B., & Swann, A. L. S. (2019). Separating the impact of individual land surface properties on the terrestrial surface energy budget in both the coupled and uncoupled land–atmosphere system. *Journal of Climate*, *32*(18), 5725–5744. doi: 10.1175/JCLI-D-18-0812.1

Laguë, M. M., Pietschnig, M., Ragen, S., Smith, T. A., & Battisti, D. S. (2021). Terrestrial evaporation and global climate: Lessons from Northland, a planet with a hemispheric continent. *Journal of Climate*, *34*(6), 2253–2276. doi: 10.1175/JCLI-D-20-0452.1

Laguë, M. M., Quetin, G. R., & Boos, W. R. (2023). Reduced terrestrial evaporation increases atmospheric water vapor by generating cloud feedbacks. *Environmental Research Letters*, *18*(7), 074021. doi: 10.1088/1748-9326/acdbe1

Laguë, M. M., Swann, A. L. S., & Boos, W. R. (2021). Radiative Feedbacks on Land Surface Change and Associated Tropical Precipitation Shifts. *Journal of Climate*, *34*(16), 6651–6672. doi: 10.1175/JCLI-D-20-0883.1

Lee, J., & Hohenegger, C. (2024). Weaker land–atmosphere coupling in global storm-resolving simulation. *Proceedings of the National Academy of Sciences*, *121*(12), e2314265121. doi: 10.1073/pnas.2314265121

Lemordant, L., Gentine, P., Swann, A. S., Cook, B. I., & Scheff, J. (2018). Critical impact of vegetation physiology on the continental hydrologic cycle in response to increasing CO2. *Proceedings of the National Academy of Sciences*, *115*(16), 4093–4098. doi: 10.1073/pnas.1720712115

Lorenz, R., Pitman, A. J., & Sisson, S. A. (2016). Does Amazonian deforestation cause global effects; can we be sure? *Journal of Geophysical Research: Atmospheres*, *121*(10), 5567–5584. doi: 10.1002/2015JD024357

Massmann, A., Gentine, P., & Lin, C. (2019). When Does Vapor Pressure Deficit Drive or Reduce Evapotranspiration? *Journal of Advances in Modeling Earth Systems*, *11*(10), 3305–3320. doi: 10.1029/2019MS001790

McColl, K. A., & Rigden, A. J. (2020). Emergent Simplicity of Continental Evapotranspiration. *Geophysical Research Letters*, *47*(6), e2020GL087101. doi: 10.1029/2020GL087101

McColl, K. A., Salvucci, G. D., & Gentine, P. (2019). Surface Flux Equilibrium Theory Explains an Empirical Estimate of Water-Limited Daily Evapotranspiration. *Journal of Advances in Modeling Earth Systems*, *11*(7), 2036–2049. doi: 10.1029/2019MS001685

Rigden, A. J., & Salvucci, G. D. (2015). Evapotranspiration based on equilibrated relative humidity (ETRHEQ): Evaluation over the continental U.S. *Water Resources Research*, *51*(4), 2951–2973. doi: 10.1002/2014WR016072

Salvucci, G. D., & Gentine, P. (2013). Emergent relation between surface vapor conductance and relative humidity profiles yields evaporation rates from weather data. *Proceedings of the National Academy of Sciences*, *110*(16), 6287–6291. doi: 10.1073/pnas.1215844110

Santanello, J. A., Dirmeyer, P. A., Ferguson, C. R., Findell, K. L., Tawfik, A. B., Berg, A., ... Wulfmeyer, V. (2018). Land–Atmosphere interactions: The LoCo perspective. *Bulletin of the American Meteorological Society*, *99*(6), 1253–1272. doi: 10.1175/BAMS-D-17-0001.1

Sellers, P. J., Bounoua, L., Collatz, G. J., Randall, D. A., Dazlich, D. A., Los, S. O., ... Jensen, T. G. (1996). Comparison of Radiative and Physiological Effects of Doubled Atmospheric CO2 on Climate. *Science*, *271*(5254), 1402–1406. doi: 10.1126/science.271.5254.1402

Seneviratne, S. I., Corti, T., Davin, E. L., Hirschi, M., Jaeger, E. B., Lehner, I., ... Teuling, A. J. (2010). Investigating soil moisture–climate interactions in a changing climate: A review. *Earth-Science Reviews*, *99*(3), 125–161. doi: 10.1016/j.earscirev.2010.02.004

Seneviratne, S. I., Koster, R. D., Guo, Z., Dirmeyer, P. A., Kowalczyk, E., Lawrence, D., ... Verseghy, D. (2006). Soil Moisture Memory in AGCM Simulations: Analysis of Global Land–Atmosphere Coupling Experiment (GLACE) Data. *Journal of Hydrometeorology*, *7*(5), 1090–1112. doi: 10.1175/JHM533.1

Seneviratne, S. I., Wilhelm, M., Stanelle, T., van den Hurk, B., Hagemann, S., Berg, A., ... Smith, B. (2013). Impact of soil moisture-climate feedbacks on CMIP5 projections: First results from the GLACE-CMIP5 experiment. *Geophysical Research Letters*, *40*(19), 5212–5217. doi: 10.1002/grl.50956

Shukla, J., & Mintz, Y. (1982). Influence of land-surface evapotranspiration on the Earth's climate. *Science*, *215*(4539), 1498–1501.

Teuling, A. J., Taylor, C. M., Meirink, J. F., Melsen, L. A., Miralles, D. G., van Heerwaarden, C. C., ... de Arellano, J. V.-G. (2017). Observational evidence for cloud cover enhancement over western European forests. *Nature Communications*, *8*(1), 14065. doi: 10.1038/ncomms14065

Tuttle, S., & Salvucci, G. (2016). Empirical evidence of contrasting soil moisture–precipitation feedbacks across the United States. *Science*, *352*(6287), 825–828. doi: 10.1126/science.aaa7185

van Heerwaarden, C. C., Vilà-Guerau de Arellano, J., Moene, A. F., & Holtslag, A. A. M. (2009). Interactions between dry-air entrainment, surface evaporation and convective boundary-layer development. *Quarterly Journal of the Royal Meteorological Society*, *135*(642), 1277–1291. doi: 10.1002/qj.431

Vargas Zeppetello, L. R., Donohoe, A., & Battisti, D. S. (2019). Does Surface Temperature Respond to or Determine Downwelling Longwave Radiation? *Geophysical Research Letters*, *46*(5), 2781–2789. doi: 10.1029/2019GL082220

Wei, J., & Dirmeyer, P. A. (2012). Dissecting soil moisture-precipitation coupling. *Geophysical Research Letters*, *39*(19). doi: 10.1029/2012GL053038

Whittaker, R. H. (1975). *Communities and Ecosystems* (2nd ed.). New York: MacMillan.

Wilks, D. S. (2016). "The Stippling Shows Statistically Significant Grid Points": How Research Results are Routinely Overstated and Overinterpreted, and What to Do about It.
doi: 10.1175/BAMS-D-15-00267.1

Zarakas, C. M., Kennedy, D., Dagon, K., Lawrence, D. M., Liu, A., Bonan, G., ... Swann, A. L. S. (2024). Land Processes Can Substantially Impact the Mean Climate State. *Geophysical Research Letters*, *51*(21), e2024GL108372. doi: 10.1029/2024GL108372

Zarakas, C. M., & Swann, A. L. S. (2025). *Community Land Model synthetic meteorology simulation model output.* Dryad. Retrieved from `https://doi.org/10.5061/dryad.h44j0zpw1` doi: 10.5061/dryad.h44j0zpw1

Zarakas, C. M., & Swann, A. L. S. (2026a). *Coupled land perturbed parameter ensemble.* Dryad. Retrieved from `http://datadryad.org/share/LINK_NOT_FOR_PUBLICATION/waLcy91bwif3a2LglSZpWhQGVSJbe_qrrZqvGush3O8` doi: 10.5061/dryad.stqjq2cf7

Zarakas, C. M., & Swann, A. L. S. (2026b). *Land-only land perturbed parameter ensemble.* Dryad. Retrieved from `http://datadryad.org/share/LINK_NOT_FOR_PUBLICATION/zvoI4LdEc_PTxp0CrR46wtAIgYXCZzPjtiy7zL1jrvA` doi: 10.5061/dryad.n8pk0p377

Zarakas, C. M., Swann, A. L. S., Laguë, M. M., Armour, K. C., & Randerson, J. T. (2020). Plant physiology increases the magnitude and spread of the transient climate response to CO2 in CMIP6 Earth system models. *Journal of Climate*, *33*(19), 8561–8578. doi: 10.1175/JCLI-D-20-0078.1

Zhang, L. N., Gianotti, D. J. S., & Entekhabi, D. (2023). Land Surface Influence on Convective Available Potential Energy (CAPE) Change during Interstorms.
doi: 10.1175/JHM-D-22-0191.1

Zhou, S., & Yu, B. (2025). Neglecting land–atmosphere feedbacks overestimates climate-driven increases in evapotranspiration. *Nature Climate Change*, *15*(10), 1099–1106. doi: 10.1038/s41558-025-02428-5

Land-Atmosphere Feedbacks Dampen Surface Evapotranspiration in Wet Regions

1 Regionally- vs. Remotely-Driven Land-Atmosphere Feedbacks

Land-atmosphere feedbacks lead global-scale land parameter perturbations to affect ET differently in a coupled context than in a land-only context. Our analysis focuses on testing whether land-atmosphere feedbacks at any spatial scale modulate changes in land surface fluxes (i.e., where is $\Delta ET_{coupled}$ different from $\Delta ET_{land-only}$). However, we note that in the coupled context, both local and remote land surface changes impact the atmosphere in a given grid cell. We use the fraction of variance explained by local regression with land-only ET changes as a proxy for the extent to which local to regional ET changes are responsible for the observed land-atmosphere feedbacks. In many tropical and temperate humid to semi-arid regions, local regression explains a large fraction of variance in the coupled PPE, suggesting a dominant role of local to regional land surface changes (Figure S1e). However in deserts and the high-latitudes, local ET changes explain less than 10% of the variance in the coupled ensemble, suggesting that the coupled ET changes in those locations are driven by atmospheric responses to remote land surface changes. This would be consistent with prior work which has shown that ET changes in mid-to-high latitudes can drive Arctic amplification (Park et al., 2020) and alter atmospheric energy transport (Laguë et al., 2019). For example, in the northern Russia example location (Figure S2c), the slope of the line of best fit is statistically significantly different from one, indicating that atmospheric responses significantly alter ET changes, and that local land-only ET changes are a poor predictor of coupled ET responses. Consequently, if one were to try to use a land-only PPE to estimate how global-scale parameter uncertainty impacts high-latitude ET fluxes, the land-only PPE would give the wrong answer. However, this linear regression only explains 27% of the variance in ET across the coupled PPE at this site, indicating that in the coupled PPE, ET is likely primarily responding to remotely-driven climate changes.

2 Potential Evapotranspiration

We calculate potential ET (PET, units of mm/s) from monthly data using the Penman-Monteith equation:

$$PET = \frac{1}{\lambda} \frac{sR^*_{net} + \frac{\rho_a c_p}{r_{ah}} D}{(1 + \frac{r_{aw}}{r_{ah}})\gamma + s} \tag{1}$$

which represents PET as a function of the net radiation at the surface minus the ground heat flux (R^*_{net} in W/m^2) and the vapor pressure deficit (D in Pa). s is the change in saturation vapor pressure per degree (Pa/K), ρ_a is the density of near-surface air (kg/m^3), and γ is the psychrometric constant. C_p and λ are the specific heat of dry air ($J/(kgK)$) and the latent heat of vaporization (J/kg), respectively. PET also depends on two resistances: r_{ah}, the aerodynamic resistance to water vapor transfer from the surface to near-surface air (s/m), and r_{aw}, the aerodynamic resistance to heat transfer from the surface to near-surface air (s/m). We calculate changes in PET to illustrate changes in atmospheric controls on ET in coupled simulations. We therefore use the default FAO (Allen et al. 1998) definitions of r_{ah} and r_{aw} for a reference crop, for which r_{aw} is 70 s/m

and r_{ah} is defined as a function of wind speed:

$$r_{ah} = \frac{ln(\frac{z_m - \frac{2}{3}h}{0.123h})ln(\frac{z_m - \frac{2}{3}h}{0.0123h})}{k^2 u_z} \tag{2}$$

where z_m is the height of wind and humidity measurements, $h = 0.12$ is the reference crop height, $k = 0.41$ is von Karman's constant, and u_z is the wind speed at height z_m.

Rearranging equation 1, we separate PET into the components due to R^*_{net} ($PET_{R^*_{net}}$) and D (PET_D):

$$PET = PET_{R^*_{net}} + PET_D \tag{3}$$

where $PET_{R^*_{net}}$ and PET_D are defined in equations 4 and 5, respectively:

$$PET_{R^*_{net}} = \frac{\frac{s}{\lambda} R^*_{net}}{(1 + \frac{r_{aw}}{r_{ah}})\gamma + s} \tag{4}$$

$$PET_D = \frac{\frac{\rho_a c_p}{\lambda r_{ah}} D}{(1 + \frac{r_{aw}}{r_{ah}})\gamma + s} \tag{5}$$

3 Atmospheric Modulation of GPP

Atmospheric modulation of photosynthesis differs from atmospheric modulation of ET in several key ways. First, land-atmosphere feedbacks have a smaller impact on GPP than on ET (Figure S1c-d). Land-only ET changes only explain about 51% of the variance in coupled ET changes while land-only GPP changes explain about 71% of the variance in coupled GPP changes (averaged globally from Figure S1). This means that land-only simulations do a better job capturing the GPP response than the ET response of a coupled system.

Second, when considering variance in ET and GPP on an absolute basis, land-atmosphere feedbacks meaningfully impact ET broadly across space globally (Figure S1a), while atmospheric modulation of GPP is most important in two regional hotspots: the Amazon and the Great Plains. These regions emerge as hotspots due to the combination of three factors: (1) the absolute GPP fluxes are large, so even modest fractional changes GPP have large impacts on absolute carbon fluxes, (2) in these regions changes in land parameters cause large changes in temperature and precipitation across the PPE (Zarakas, Kennedy, et al., 2024), and (3) GPP is sensitive to temperature and precipitation in these regions (Figure S7).

Finally, ET and GPP differ in how consistent land-atmosphere feedbacks are across the PPE. For ET, there is spatial variation in how land-atmosphere feedbacks modulate ET changes, but for any given location the direction of land-atmosphere feedbacks are quite consistent (i.e., consistently dampening or consistently amplifying ET changes), regardless of what parameter drove the initial ET change (Figure S8a-d). Because of this, the line of best fit relating $\Delta ET_{coupled}$ and $\Delta ET_{land-only}$ is statistically different from one across 57% of the land surface. Estimating $\Delta ET_{coupled}$ as a linear function of $\Delta ET_{land-only}$ (i.e., $\Delta ET_{coupled} = m * \Delta ET_{land-only}$) explains additional variance in $\Delta ET_{coupled}$ across the ensemble, particularly in wet regions (Figure S1g). In contrast, atmospheric modulation of GPP is more parameter dependent (Figure S8). Because of this, estimating $\Delta GPP_{coupled}$ as a linear function of $\Delta GPP_{land-only}$ does not meaningfully improve the amount of $\Delta GPP_{coupled}$ variance explained (Figure S1h).

The impact of land-atmosphere feedbacks on GPP is parameter-dependent because GPP does not directly impact the atmosphere in our experimental design, due to the fact that our simulations include only biogeophysical feedbacks, rather than biogeochemical

feedbacks (i.e., atmospheric CO_2 is held constant). Land-atmosphere feedbacks therefore modulate GPP changes only if a parameter perturbation impacts both GPP and land surface properties, and then those land surface properties impact the atmosphere, which feeds back on GPP. In both the Amazon and the Great Plains, the parameter dependent impact of land-atmosphere feedbacks on GPP can be explained by differences across parameters in the relationship between GPP and ET changes: land-atmosphere feedbacks amplify GPP changes when a parameter increases (or decreases) both GPP and ET in tandem, and land-atmosphere feedbacks dampen GPP or drive sign changes when a parameter modifies GPP and ET in opposite directions (Figure S9).

For example, in the Amazon, increasing the maximum hydraulic conductance of plants (`kmax`) both increases evapotranspiration and increases GPP, because photosynthesis in the default case is limited by leaf water potential, and increased stem hydraulic conductance enables available water in deep soil layers to be transported to the leaves of trees. The atmosphere directly responds to `kmax`'s influence on ET, leading to decreases in regional temperature and vapor pressure deficit. This atmospheric feedback dampens ET changes, but amplifies GPP changes because decreasing temperature increases photosynthetic rates in the tropics (Figure S7d). We note that in CESM, this temperature sensitivity is not due to direct temperature effects on photosynthesis, but rather due to the fact that decreasing temperature decreases VPD, and lower VPD increases stomatal conductance which thereby increases photosynthesis (Zarakas, Swann, et al., 2024). Atmospheric amplification of `kmax`'s influence on GPP is consistent with prior work that hypothesized that the evolution of angiosperms (which have higher hydraulic conductance) enhance photosynthesis in the Amazon (Lee & Boyce, 2010).

Most parameter perturbations cause ET and GPP to change in the same direction like `kmax`, but some parameters change the coupling of ET and GPP. In both the Amazon and the Great Plains parameters influencing stomatal conductance change the coupling between ET and GPP by changing leaf-level trade-offs between carbon gain and water loss (Figure S9). For example, increasing `medlynintercept` increases ET but decreases GPP. The ET increase drives the same climate responses in the Amazon as increasing `kmax` does, which increase GPP, but this acts to counter the initial GPP change, so the land-atmosphere feedback is dampening. In the Great Plains, parameters which influence the partitioning between soil evapotranspiration, canopy evaporation, and transpiration (Figure S10) also modify the coupling of ET and GPP (Figure S9).

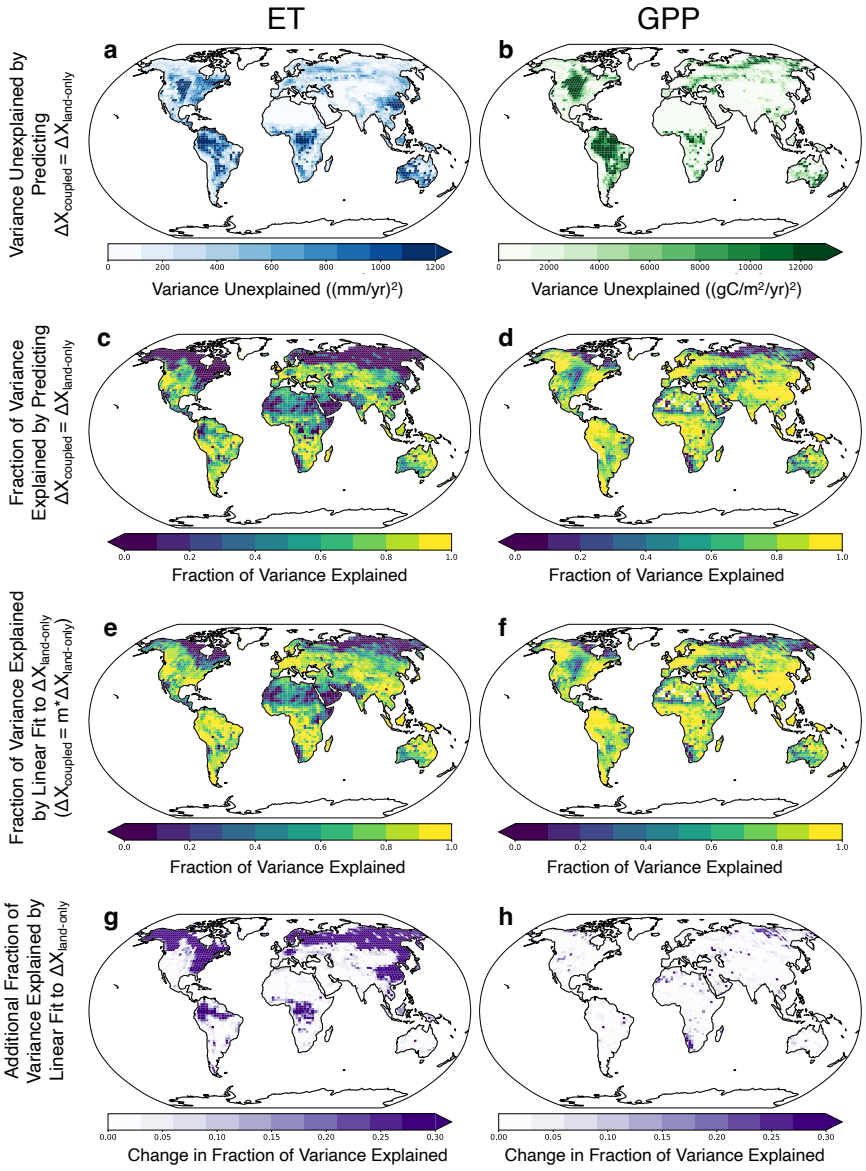

Figure S1. Comparison of variance in changes in coupled ET (left) and GPP (right) explained by the land-only PPE. Top row shows the variance unexplained by predicting $\Delta ET_{coupled} = \Delta ET_{land-only}$ (a) and $\Delta GPP_{coupled} = \Delta GPP_{land-only}$ (b). For ET, this is calculated as $\frac{\sum_i (\Delta ET_{coupled} - \Delta ET_{land-only})^2}{n-1}$ for all ensemble members i. Panels (c) and (d) show the *fraction* of variance explained by assuming $\Delta ET_{coupled} = \Delta ET_{land-only}$ (c) and $\Delta GPP_{coupled} = \Delta GPP_{land-only}$ (d). Panels (e) and (f) show the fraction of variance explained by the linear fit of coupled changes to land-only changes. Panels (g) and (h) how much the linear regression increases the fraction of variance explained, compared to assuming the coupled changes will equal the land-only changes.

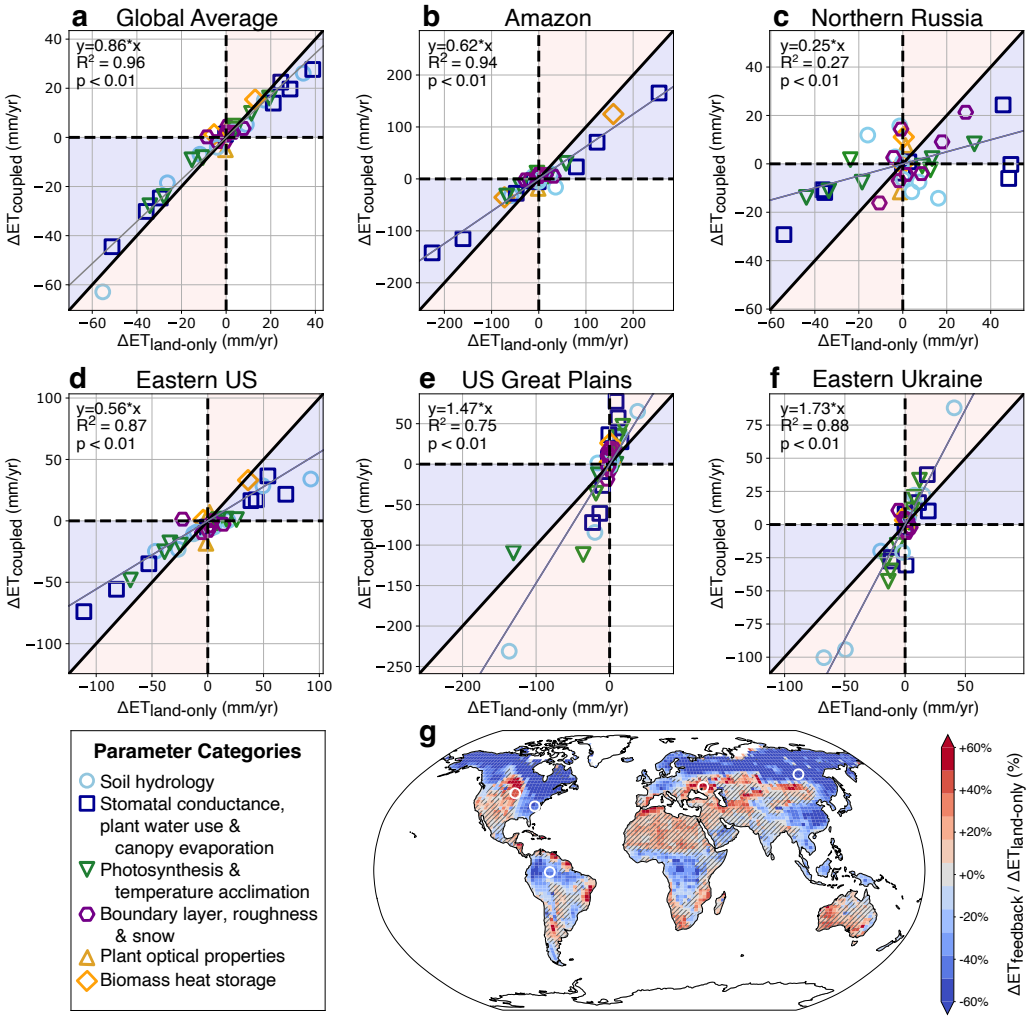

Figure S2. Relationship between land only and coupled changes in evapotranspiration, globally (a) and for several example locations (b-f), as indicated in (g). Each point is a different paired ensemble member (n = 36), and color indicates the parameter category. The parameter perturbations and categories are described in Table S1. Shading indicates whether land-atmosphere feedbacks amplify (red) or dampen (blue) evapotranspiration changes. The thick black line indicates the 1:1 line dividing amplifying and dampening feedbacks, and the thin gray line indicates the line of best fit, calculated via ordinary least squares linear regression with y-intercept=0. p-values indicate whether slopes are statistically significantly different from 1.

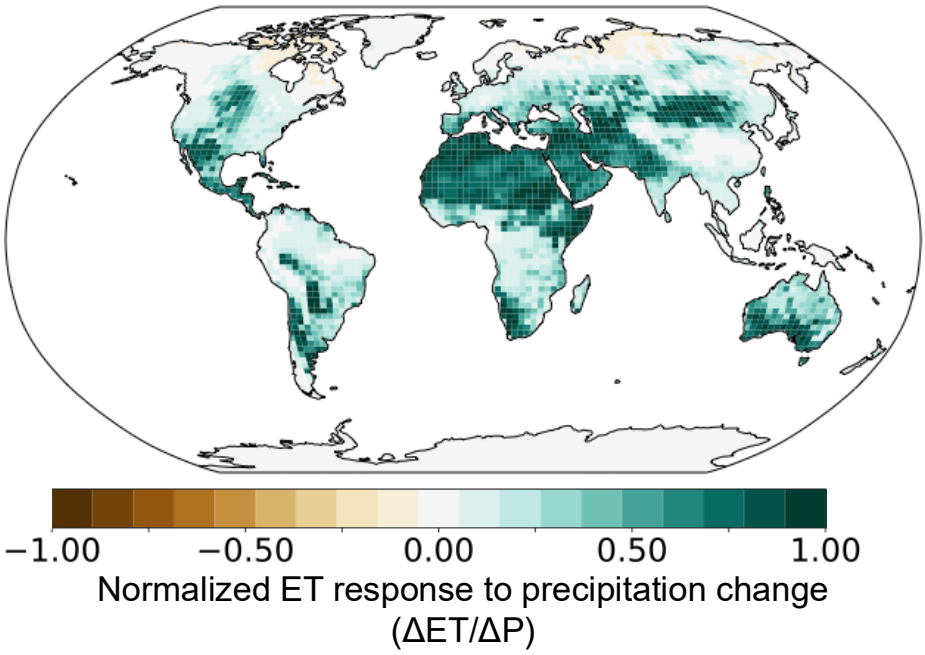

Figure S3. How precipitation changes impact ET. ET response to idealized 10% precipitation increase. The idealized meteorological treatment is described in section 2.2.3. This data is the same as in Figure 2a, but here ET is normalized by the precipitation change to account for different magnitudes of precipitation perturbations in different regions. When the ratio is 1, all additional precipitation added is evaporated. When the ratio is 0, additional precipitation does not lead to any additional evapotranspiration. Small negative responses in the high latitudes are likely due to feedbacks driven by increases in the snow pack.

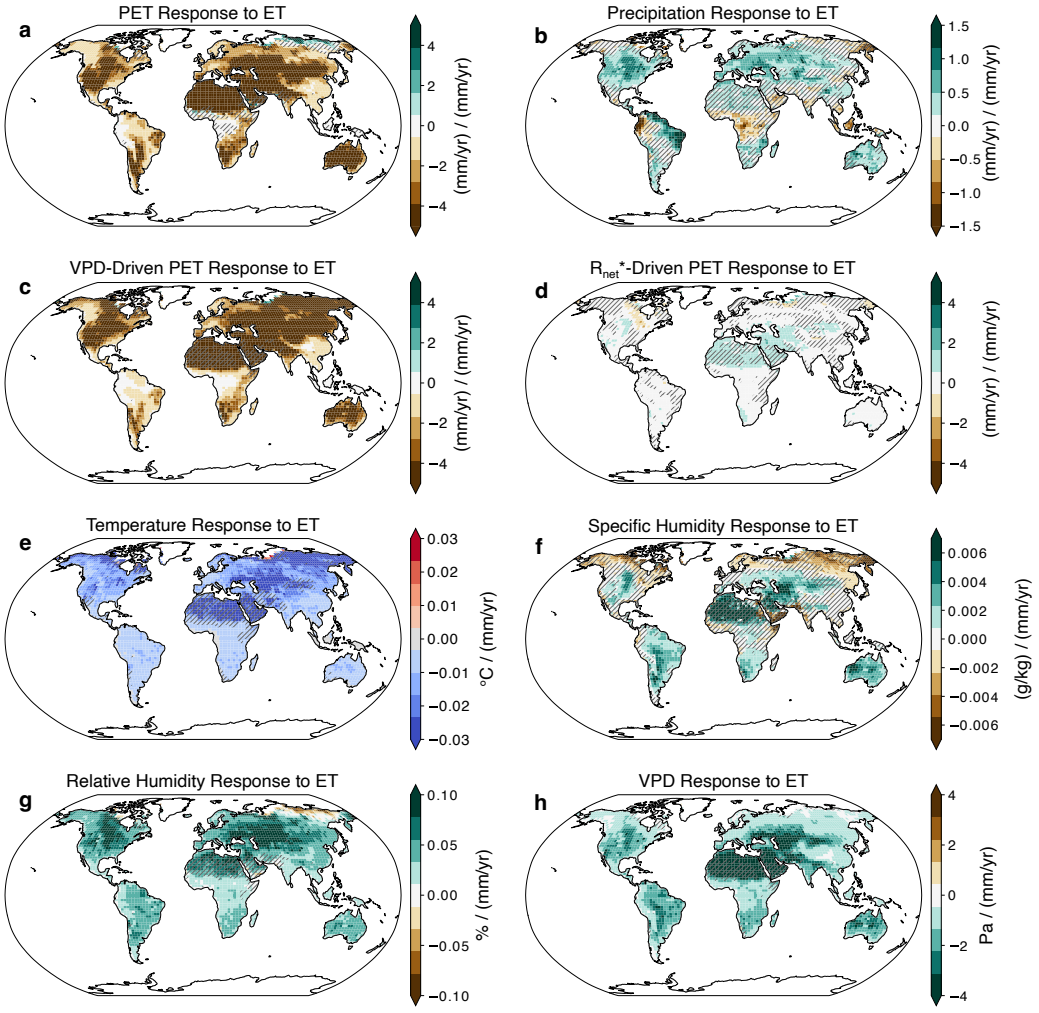

Figure S4. How ET influences the atmosphere. Sensitivity of various quantities to ET, quantified by linear regression. Positive values indicate that increasing evapotranspiration increases the atmospheric variable. Stippling indicates regions where the slope is not statistically significantly different from 0. An increase in ET drives (a) a decrease in PET and (b) regionally variable changes in precipitation. The PET change in (a) is mostly driven by changes in the VPD component of PET (c), with minimal contributions from the R^*_{net} component (d). Sensitivity of (e) air temperature, (f) specific humidity, (g) relative humidity, and (h) vapor pressure deficit, VPD, to changes in ET. Increasing ET decreases temperature globally (e), and increases specific humidity in some low- and mid-latitude regions (f). This leads to a global increase in relative humidity (g) and decrease in VPD (h).

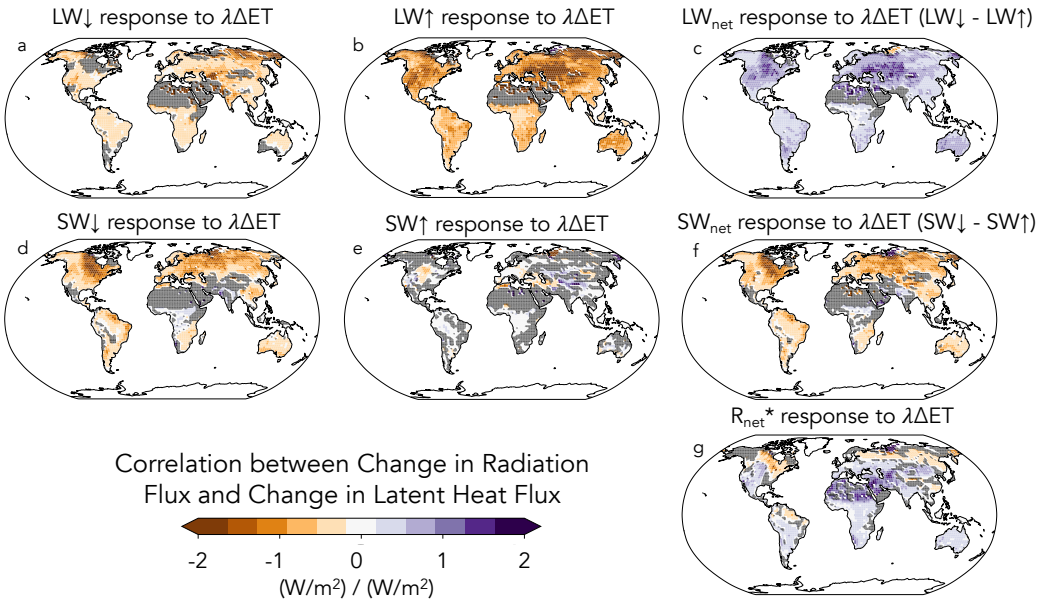

Figure S5. Influence of evapotranspiration on net radiation. Sensitivity of surface energy fluxes to changes in evapotranspiration, as in Figure 3. Increasing evapotranspiration decreases upwelling longwave, LW↑, (b) and decreases downwelling longwave, LW↓ by a smaller amount (a), leading to an increase in the net longwave flux from the atmosphere to land (c). Increasing evapotranspiration also increases downwelling shortwave, SW↓, (d) and drives small changes in upwelling shortwave, SW↑ (e), leading to a net increase in net shortwave absorbed by the land surface (f). The combined changes in longwave and shortwave radiation result in small, spatially variable changes in net radiation minus storage (R_{net}).

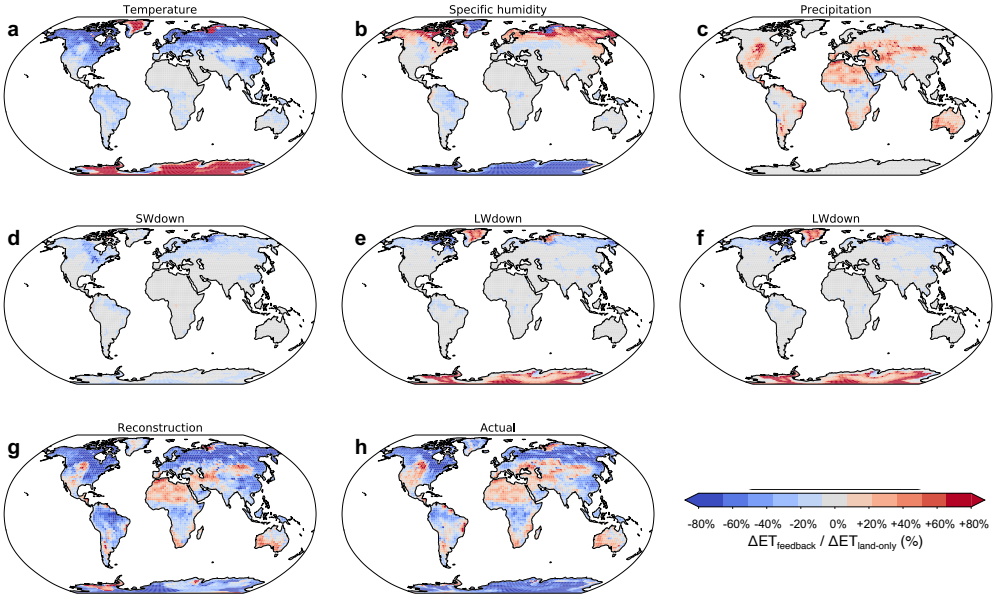

Figure S6. Linear decomposition of the atmospheric modulation of ET changes. Atmospheric modulation of ET changes due to (a) temperature, (b) specific humidity, (c) precipitation, (d) downwelling shortwave, and (e) downwelling longwave). The reconstructed atmospheric modulation of ET changes in (f) is the sum of the components in (a-e). The actual atmospheric modulation from Figure 1 is reproduced here for comparison.

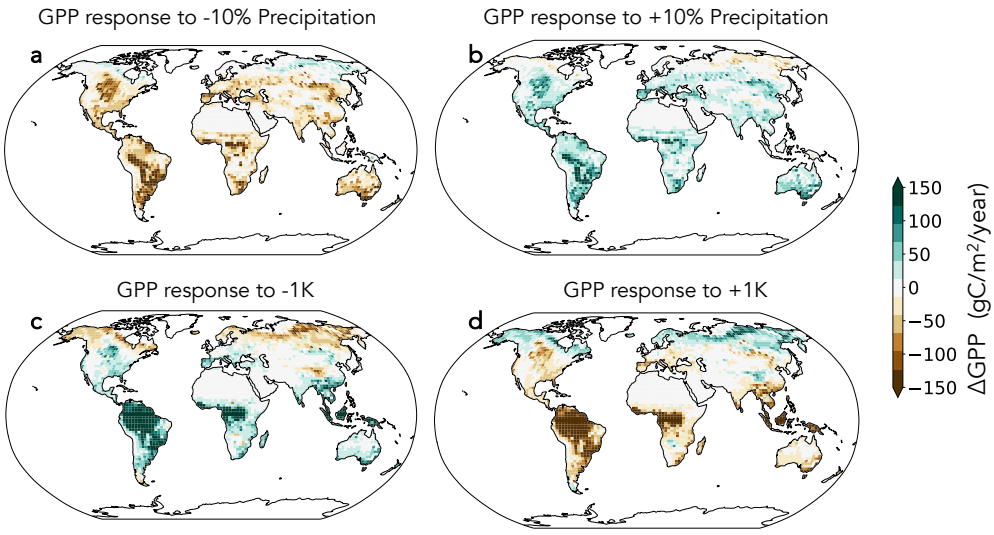

Figure S7. How atmospheric changes impact GPP. GPP (W/m^2) response to idealized meteorological treatments of (a) decreasing precipitation, (b) increasing precipitation, (c) decreasing temperature, and (d) increasing temperature.

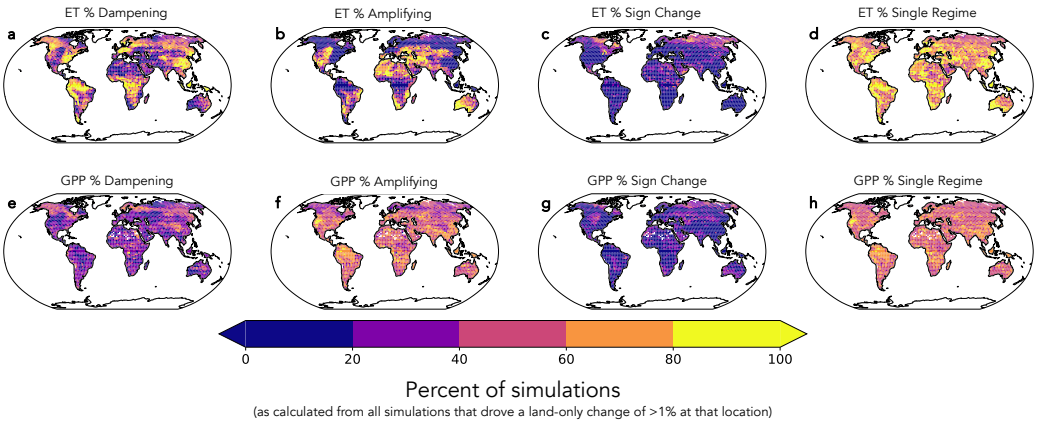

Figure S8. Consistency in the sign of atmospheric feedbacks across the PPE, for ET (top row) and GPP (bottom row). For ET, there is spatial variation in whether atmospheric feedbacks dampen (a) or amplify (b) ET changes, but for a given location atmospheric feedbacks tend to have a consistent sign of change across the PPE. We define atmospheric feedbacks as being consistent when atmospheric feedbacks drive the same qualitative impact (i.e., dampening, amplifying, or driving a sign change) across more than 80% of the PPE. For ET, about 15% of the land surface experiences consistent dampening feedbacks (a), and 11% of the land experiences consistent amplifying feedbacks (b), leading to consistent signs of change for 26% of the land surface (d). For GPP, there is less spatial variation in whether atmospheric feedbacks dampen or amplify GPP changes, but at a given location atmospheric feedbacks are less consistent (i.e., atmospheric feedbacks are parameter dependent). Essentially none of the land surface experiences consistent dampening feedbacks, and less than 2% of land experiences consistent amplifying feedbacks.

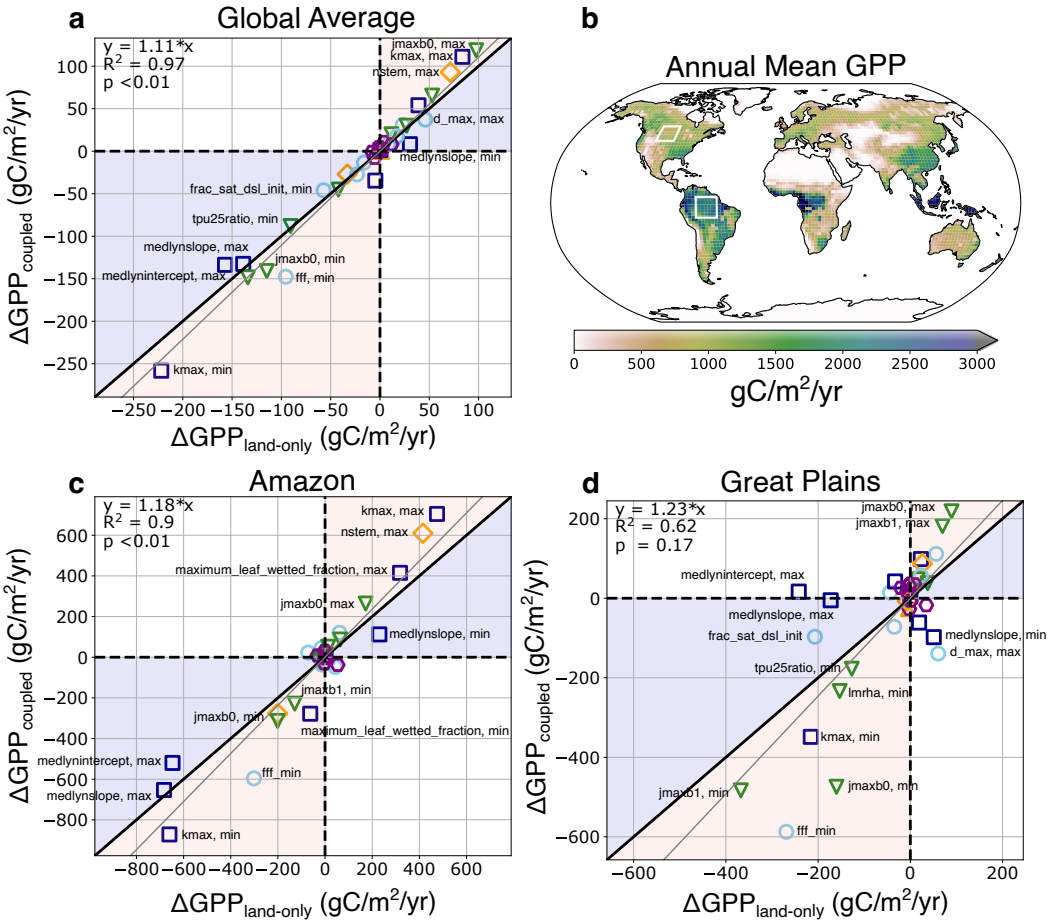

Figure S9. Relationship between land-only and coupled changes in gross primary production. As in Figure S2, but for gross primary production (GPP), averaged globally (a) and averaged across regional land-atmosphere feedback hotspots in the Amazon (c) and Great Plains (d). The regions in (c) and (d) are indicated in panel (b).

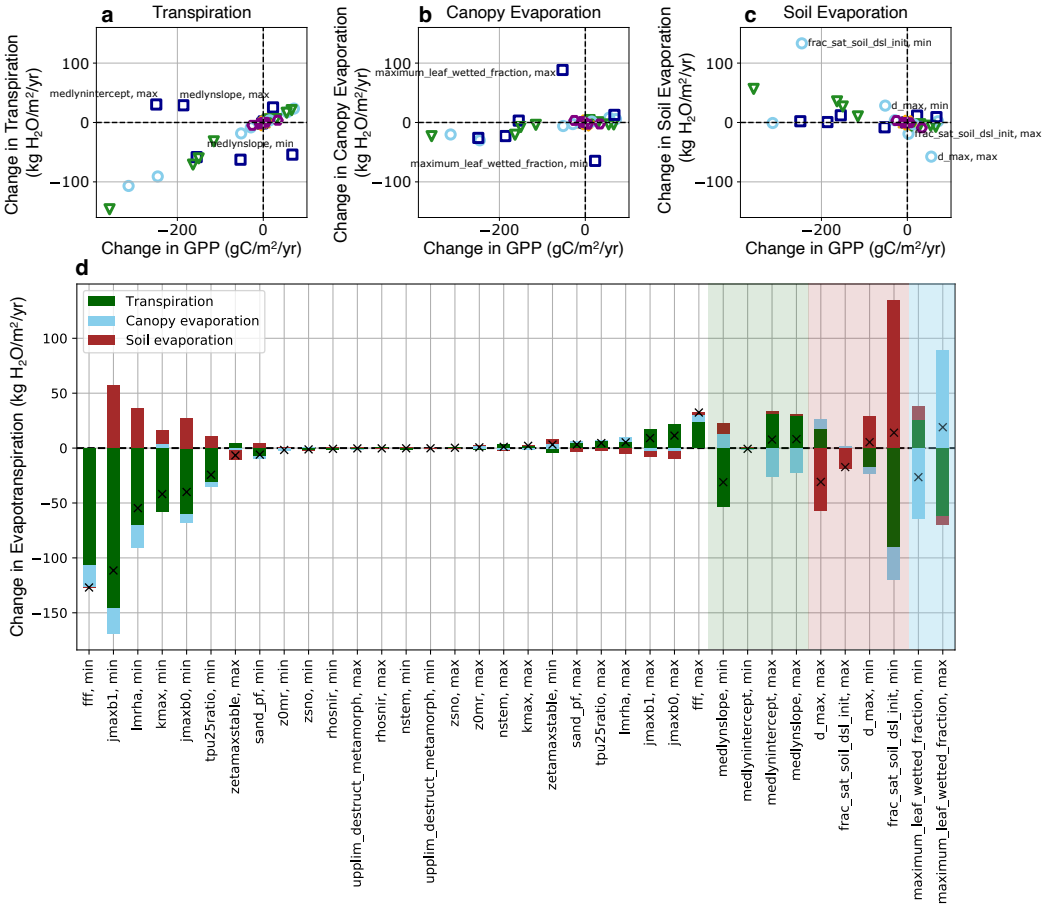

Figure S10. Relationship between parameter perturbations and different components of the total evapotranspiration flux in the Great Plains. Top row shows the relationship between land-only changes in GPP and land-only changes in transpiration (a), canopy evaporation (b), and soil evaporation (c). The bottom row indicates how parameter perturbations impact different components of evapotranspiration. Highlighted parameters on the right indicate stomatal conductance parameter perturbations (green), dry surface layer parameter perturbations (red), and perturbations which directly influence canopy evaporation rates (blue).

Parameter	Parameter description	Land component	Parameter category	Min value	Default value	Max value	Unit	Range source
d_max	Parameter specifying the length scale of max dry surface layer thickness	Soil	Soil hydrology	10	15	60	mm	Literature review
frac_sat_soil_dsl_init	Fraction of saturated soil for moisture value at which dry surface layer initiates			0.5	0.8	1	unitless	Literature review
fff	Decay factor for fractional saturated area			0.02	0.5	5	m^{-1}	Literature review
sand_pf	Perturbation factor (via addition) for percent sand			-20	0	20	percent	% perturbation
z_0mr	Ratio of momentum roughness length to canopy top height	Boundary layer	Boundary layer / roughness length	0.033 to 0.072[a]	0.055 to 0.120[a]	0.077 to 0.168[a]	unitless	Literature review
z_sno	Momentum roughness length for snow			0.00001	0.0024	0.07	m	Literature review
zetamaxstable	Max value zeta ("height" used in Monin- Obukhov theory) can go to under stable conditions.*			0.1	0.5	10	unitless	Expert judgement
upplim_destruct_metamorph	Upper limit for snow densification through destructive metamorphism		Snow	100	175	250	kg/m^2	Literature review
jmaxb0	Tthe baseline proportion of nitrogen allocated for electron transport	Vegetation	Photosynthesis	0.01	0.0311	0.05	J	Expert judgement
jmaxb1	Determines the response of electron transport rate to light availability			0.05	0.17	0.25	unitless	Expert judgement
tpu25ratio	Triose phosphate utilization at 25C (ratio of tpu25/vcmax25)			0.0835	0.167	0.501	unitless	% perturbation
lmrha	Activation energy for leaf maintenance respiration (used in temperature acclimation of leaf maintenance respiration)		Temperature acclimation	-50%	46390	+50%	J/mol	% perturbation

Parameter	Parameter description	Land component	Parameter category	Min value	Default value	Max value	Unit	Range source
medlynslope	Medlyn slope of conductance-photosynthesis relationship	Vegetation	Stomatal conductance and plant water use	0.65 to 3.89[a]	1.62 to 5.79[a]	3.93 to 9.11[a]	μmol H_2O /μmol CO_2	Literature review
medlynintercept	Medlyn intercept of conductance-photosynthesis relationship			1	100	200000	μmol H_2O /m^2/s	Literature review
kmax	Plant segment maximum conductance			2.3e-10 to 1.5e-8[a]	1.3e-9 to 4.0e-8[a]	1.9e-9 to 2.3e-7[a]	mm H_2O (transpired) /mm H_2O (water potential gradient) / s	Literature review
rhosnir	Near-infrared stem reflectance		Plant optical properties	0.29 to 0.42[a]	0.36 to 0.53[a]	0.43 to 0.64[a]	unitless	% perturbation
maximum_leaf_wetted_fraction	Maximum fraction of leaf that may be wet prior to drip occuring		Canopy evaporation	0.01	0.05	0.5	unitless	Expert judgement
nstem	Stem number; number of individuals per meter squared (similar to stocking number). Influences canopy height and biomass heat storage.		Canopy height / biomass heat storage	0.03	0.035 to 100[a]	0.5	number/m^2	Expert judgement

Table S1. List of parameters. This table is adapted from (Zarakas, Kennedy, et al., 2024), reporting parameter ranges developed by (Kennedy et al., 2025)

[a]Parameter ranges vary depending on the plant functional type.

Category	Field
Temperature	Temperature at lowest atmospheric level Potential temperature at lowest atmospheric level
Precipitation	Liquid precipitation Solid precipitation
Humidity	Specific humidity
Surface radiation	Incident direct beam visible solar radiation Incident direct beam near-infrared solar radiation Incident diffuse visible solar radiation Incident diffuse near-infrared solar radiation Incident longwave radiation
Wind	Zonal wind at atmospheric reference height Meridional wind at atmospheric reference height
Height and pressure	Atmospheric reference height Atmosphere model's surface height Pressure
Biogeochemistry	Carbon dioxide (CO_2) concentration* Nitrogen deposition rate* Lightning frequency* Aerosol deposition rate

Table S2. Atmospheric inputs to the land model in CESM. Adapted from Table 2.4 in the Community Land Model Version 5 Technical Note. *These quantities cannot change in our model configuration

Simulation	Variable	Variable description	Perturbation
Increase temp	a2x3h_Sa_tbot	Temperature at the lowest model level	+1 K
Decrease temp	a2x3h_Sa_tbot	Temperature at the lowest model level	-1 K
Increase precip	a2x3h_Faxa_rainl a2x3h_Faxa_rainc a2x3h_Faxa_snowl a2x3h_Faxa_snowc	Large-scale precipitation rate Convective precipitation rate Large scale snow rate Convective snow rate	+10% +10% +10% +10%
Decrease precip	a2x3h_Faxa_rainl a2x3h_Faxa_rainc a2x3h_Faxa_snowl a2x3h_Faxa_snowc	Large-scale precipitation rate Convective precipitation rate Large scale snow rate Convective snow rate	-10% -10% -10% -10%
Increase SW_{down}	a2x1hi_Faxa_swndr a2x1hi_Faxa_swvdr a2x1hi_Faxa_swndf a2x1hi_Faxa_swvdf	Direct near-infrared incident solar radiation Direct visible incident solar radiation Diffuse near-infrared incident solar radiation Diffuse visible incident solar radiation	+10% +10% +10% +10%
Increase LW_{down}	a2x3h_Faxa_lwdn	Downward longwave heat flux	+10%
Increase humidity	a2x3h_Sa_shum	Specific humidity at the lowest model level	+10%

Table S3. Idealized land-only simulations.

References

Kennedy, D., Dagon, K., Lawrence, D. M., Fisher, R. A., Sanderson, B. M., Collier, N., ... Wood, A. W. (2025). One-at-a-Time Parameter Perturbation Ensemble of the Community Land Model, Version 5.1. *Journal of Advances in Modeling Earth Systems*, *17*(8), e2024MS004715. doi: 10.1029/2024MS004715

Laguë, M. M., Bonan, G. B., & Swann, A. L. S. (2019). Separating the impact of individual land surface properties on the terrestrial surface energy budget in both the coupled and uncoupled land–atmosphere system. *Journal of Climate*, *32*(18), 5725–5744. doi: 10.1175/JCLI-D-18-0812.1

Lee, J.-E., & Boyce, K. (2010). Impact of the hydraulic capacity of plants on water and carbon fluxes in tropical South America. *Journal of Geophysical Research: Atmospheres*, *115*(D23). doi: 10.1029/2010JD014568

Park, S.-W., Kim, J.-S., & Kug, J.-S. (2020). The intensification of Arctic warming as a result of CO2 physiological forcing. *Nature Communications*, *11*(1), 2098. doi: 10.1038/s41467-020-15924-3

Zarakas, C. M., Kennedy, D., Dagon, K., Lawrence, D. M., Liu, A., Bonan, G., ... Swann, A. L. S. (2024). Land Processes Can Substantially Impact the Mean Climate State. *Geophysical Research Letters*, *51*(21), e2024GL108372. doi: 10.1029/2024GL108372

Zarakas, C. M., Swann, A. L. S., Koven, C. D., Smith, M. N., & Taylor, T. C. (2024). Different model assumptions about plant hydraulics and photosynthetic temperature acclimation yield diverging implications for tropical forest gross primary production under warming. *Global Change Biology*, *30*(9), e17449. doi: 10.1111/gcb.17449